



The following Communications have been judged by at least two referees to be “very important papers” and will be published online at www.angewandte.org soon:

A. Patzer, M. Schütz, T. Möller, O. Dopfer*

Infrared Spectrum and Structure of the Adamantane Cation: Direct Evidence for Jahn–Teller Distortion

D. Globisch, C. A. Lowery, K. C. McCague, K. D. Janda*

Uncharacterized 4,5-Dihydroxy-2,3-Pentanedione Molecules Revealed Through NMR Spectroscopy: Implications for a Greater Signaling Diversity in Bacterial Species

C. Parthier, S. Görlich, F. Jaenecke, C. Breithaupt, U. Bräuer, U. Fandrich, D. Clausnitzer, U. F. Wehmeier, C. Böttcher, D. Scheel, M. T. Stubbs*

The O-Carbamoyl Transferase TobZ Catalyzes an Ancient Enzymatic Reaction

C. Giese, F. Zosel, C. Puorger, R. Glockshuber*

The Most Stable Protein/Ligand Complex: Applications for One-Step Affinity Purification and Identification of Protein Assemblies

C. Lux, M. Wollenhaupt, T. Bolze, Q. Liang, J. Köhler, C. Sarpe, T. Baumert*

Circular Dichroism in the Photoelectron Angular Distributions of Camphor and Fenchone from Multiphoton Ionization with Femtosecond Laser Pulses

X.-F. Xiong, Q. Zhou, J. Gu, L. Dong, T.-Y. Liu, Y.-C. Chen*

Trienamine Catalysis of 2,4-Dienones: Development and Application in Asymmetric Diels–Alder Reactions

M. T. C. Walvoort, H. v. d. Elst, O. J. Plante, L. Kröck, P. H. Seeberger, H. S. Overkleeft, G. A. van der Marel, J. D. Codée
Automated Solid-Phase Synthesis of β -Mannuronic Acid Alginates

P. G. Schiro, M. Zhao, J. S. Kuo, K. M. Koehler, D. E. Sabbath, D. T. Chiu*

Sensitive and High-Throughput Isolation of Rare Cells from Peripheral Blood with Ensemble-Decision Aliquot Ranking



“If I were not a scientist, I would be a chef or sommelier. My favorite place on earth is the summit of any mountain ...”

This and more about Warren E. Piers can be found on page 3514.

Author Profile

Warren E. Piers _____ 3514



D. Milstein



R. Shintani



H. Schwarz



S. Hell



P. Schwill

News

Israel Prize:

D. Milstein _____ 3515

Merck–Banyu Lectureship Award:

R. Shintani _____ 3515

Also in the News:

H. Schwarz, S. Hell und P. Schwill _____ 3515

Books

Crystal Engineering

Gautam R. Desiraju, Jagadese J. Vittal, Arunachalam Ramanan

reviewed by D. Braga _____ 3516

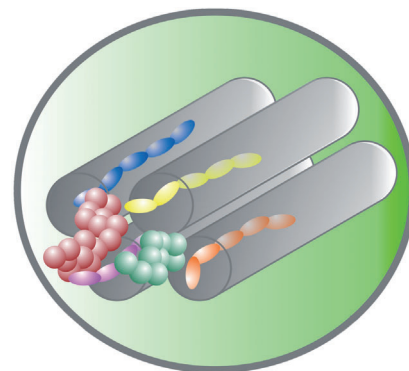
Highlights

Mesoporous Materials

F. Li, B. Dever, H. Zhang, X.-F. Li,
X. C. Le* ————— 3518–3519

Mesoporous Materials in Peptidome
Analysis

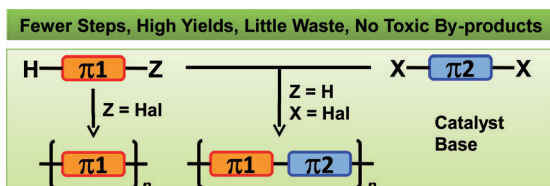
Peptide profiles: The use of mesoporous materials, such as ordered mesoporous carbon, improves the efficiency and selectivity of peptide extraction for profiling complicated samples. Controlling the pore size of such mesoporous materials during synthesis allows specific molecular weight cut-offs to be introduced, which can eliminate a large number of interfering entities, such as serum proteins.



π -Conjugated Polymers

A. Facchetti,* L. Vaccaro,
A. Marrocchi ————— 3520–3523

Semiconducting Polymers Prepared by
Direct Arylation Polycondensation



Two flavors of π : Semiconducting π -conjugated polymers may open new opportunities for the fabrication of ecofriendly, inexpensive optoelectronic devices. These

materials can be prepared by direct arylation polycondensation, a straightforward approach that generates little waste and no toxic by-products.

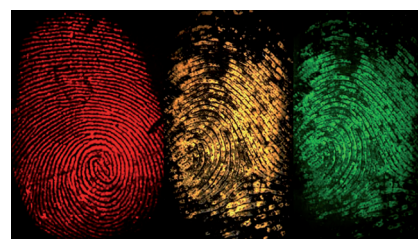
Minireviews

Fingerprinting

P. Hazarika, D. A. Russell* – 3524–3531

Advances in Fingerprint Analysis

Reading the small print: The detection of analytes of forensic importance such as drugs of abuse and explosives from a person's fingerprint together with the ability to identify that person is an important development in forensic science. This Minireview highlights the advances in this area of research, such as the use of nanoparticles, magnetic particles, quantum dots, as well as mass spectrometry, and spectroscopy.



For the USA and Canada:
ANGEWANDTE CHEMIE International
Edition (ISSN 1433-7851) is published weekly
by Wiley-VCH, PO Box 191161, 69451 Wein-
heim, Germany. Air freight and mailing in the
USA by Publications Expediting Inc., 200
Meacham Ave., Elmont, NY 11003. Periodicals

postage paid at Jamaica, NY 11431. US POST-
MASTER: send address changes to *Angewandte
Chemie*, Journal Customer Services, John
Wiley & Sons Inc., 350 Main St., Malden,
MA 02148-5020. Annual subscription price for
institutions: US\$ 11,738/10,206 (valid for print
and electronic / print or electronic delivery); for

individuals who are personal members of
a national chemical society prices are available
on request. Postage and handling charges
included. All prices are subject to local VAT/
sales tax.

Reviews

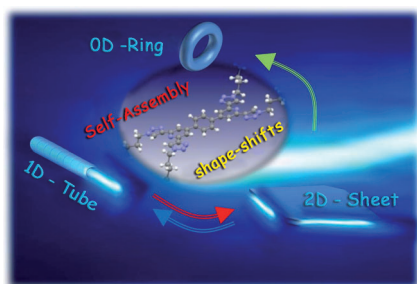
The art of sensorship: Fluorescence imaging methods in combination with optical chemical sensors enable the visualization of flows on surfaces (see picture), temperature gradients, and the two-dimensional distribution of certain chemical species (O_2 , H^+ , metal ions, H_2O_2) at an interface. This Review highlights the design of sensor materials, including nanoprobess, and the development of multiple sensors and their signal readout.



Chemical Sensors

M. Schäferling* — 3532 – 3554

The Art of Fluorescence Imaging with Chemical Sensors



Shape-shifting: A method for reversibly transforming the shape of organic waveguides to form 2D nanosheets, 1D nanotubes, and 0D nanorings has been developed. The nanosheets can be turned into nanotubes and subsequently into nanorings by adding water to the solvent, whereas ultrasonication changes the nanotubes back into nanosheets. Both nanotubes and nanosheets act as waveguides and change the direction of incident laser light in a shape-dependent manner.

Communications

Nanostructures

N. Chandrasekhar,
R. Chandrasekar* — 3556 – 3561

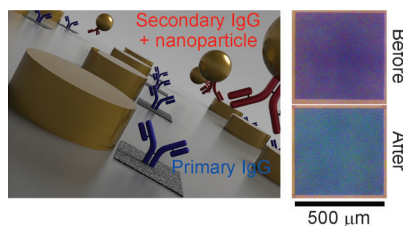
Reversibly Shape-Shifting Organic Optical Waveguides: Formation of Organic Nanorings, Nanotubes, and Nanosheets



Frontispiece



Naked-eye detection: The versatility of direct-write nanolithography was combined with the unrivaled resolution and selectivity of molecular self-assembly to show, for the first time, the molecularly mediated placement, with nanometer accuracy, of single Au nanoparticles within a plasmonic array. In doing so, a coupled plasmonic systems was created which allowed colorimetric, naked-eye detection of protein–protein binding at extreme sensitivities.



Biosensors

A. W. Clark, J. M. Cooper* — 3562 – 3566

Plasmon Shaping by using Protein Nanoarrays and Molecular Lithography to Engineer Structural Color



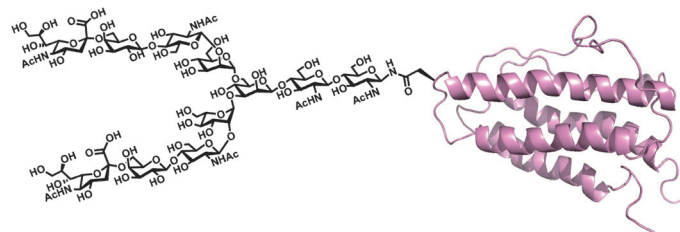
Front Cover





Glycoprotein Synthesis

M. Murakami, R. Okamoto, M. Izumi,
Y. Kajihara* 3567–3572



New and improved: New reaction conditions for *tert*-Boc-based solid-phase peptide synthesis make acid-labile sialyl-oligosaccharyl peptide α -thioesters

accessible. To demonstrate this, a sialyl-oligosaccharyl-erythropoietin glycoform (see picture) with 166 amino acid residues was synthesized.



Chemical Synthesis of an Erythropoietin Glycoform Containing a Complex-type Disialyloligosaccharide



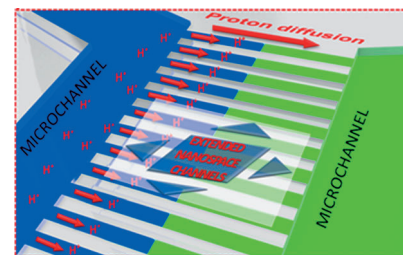
Inside Cover



Proton Mobility

H. Chinen, K. Mawatari, Y. Pihosh,
K. Morikawa, Y. Kazoe, T. Tsukahara,
T. Kitamori* 3573–3577

Channeling of mobility: A new method for the direct measurement of proton mobilities based on a pH-sensitive fluorescence probe is described. The results verify the enhancement of proton mobility in two-dimensional extended nanospace channels and contribute to a deeper understanding of ion-transport processes inside nanochannels.



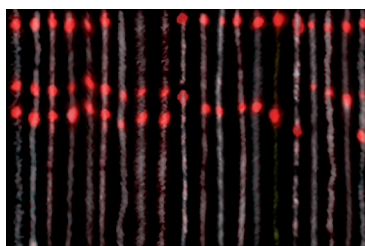
Enhancement of Proton Mobility in Extended-Nanospace Channels



Inside Back Cover

Genomic Imaging

S. Kim, A. Gottfried, R. R. Lin, T. Dertinger,
A. S. Kim, S. Chung, R. A. Colyer,
E. Weinhold,* S. Weiss,*
Y. Eberstein* 3578–3581



All smiles: Sequence-specific methyltransferase-induced labeling of DNA (SMiling DNA) creates a fluorescence pattern of the T7 bacteriophage genome (see picture). The pattern is visualized as a linear optical barcode showing the genomic location of individual RNA polymerases bound to the DNA. The precision of the measurement presents new opportunities for contextual genomic research on the single-molecule level.



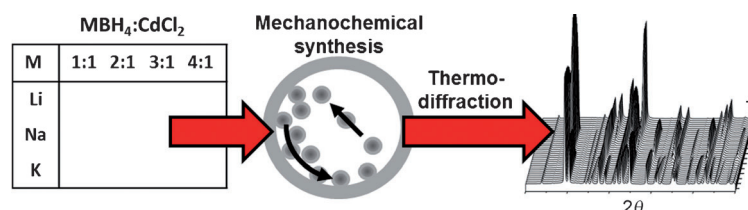
Enzymatically Incorporated Genomic Tags for Optical Mapping of DNA-Binding Proteins



Back Cover

Unstable Borohydrides

D. B. Ravnsbæk, L. H. Sørensen,
Y. Filinchuk,* F. Besenbacher,
T. R. Jensen* 3582–3586



Ay, there's the rub: The formation of cadmium-based borohydrides is screened by mechanochemical synthesis using various reactants in different ratios. Sequential in situ variable-temperature diffraction

studies provide simultaneous information about composition, structure, decomposition pathways, and properties of the compounds.



Rattling the cage: The rapid one-pot double 1,3-dipolar cycloaddition reaction of the rare endohedral fullerene $N@C_{60}$ to an oligo(*p*-phenylene polyethylene) bis-(aldehyde) using a novel amino acid derivative as an anchoring group is reported. The method provides the first example of a chemically linked, two-spin-center $N@C_{60}$ - $N@C_{60}$ molecule (see picture). Assessment of this platform as an element of a quantum computing register is attractive.

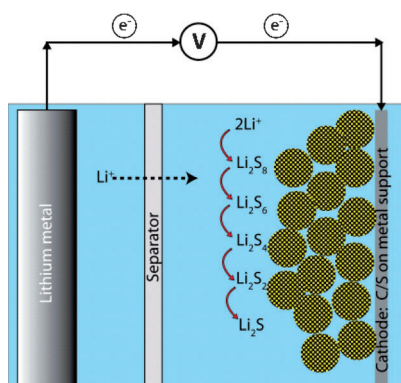
Cage Compounds

B. J. Farrington, M. Jevric, G. A. Rance, A. Ardavan, A. N. Khlobystov, G. A. D. Briggs, K. Porfyrakis* ————— 3587 – 3590

Chemistry at the Nanoscale: Synthesis of an $N@C_{60}$ - $N@C_{60}$ Endohedral Fullerene Dimer



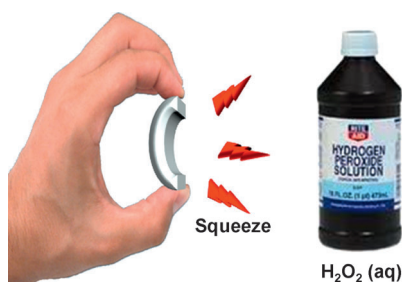
Superior cathode material: Spherical ordered mesoporous carbon nanoparticles featuring very high inner porosity (pore volume of $2.32 \text{ cm}^3 \text{ g}^{-1}$ and surface area of $2445 \text{ m}^2 \text{ g}^{-1}$) were synthesized in a two-step casting process. They were successfully applied as cathode material in Li-S batteries, where they showed high reversible capacity up to 1200 mAh g^{-1} and excellent cycling efficiency.



Lithium-Sulfur Battery

J. Schuster, G. He, B. Mandlmeier, T. Yim, K. T. Lee, T. Bein,* L. F. Nazar* ————— 3591 – 3595

Spherical Ordered Mesoporous Carbon Nanoparticles with High Porosity for Lithium-Sulfur Batteries

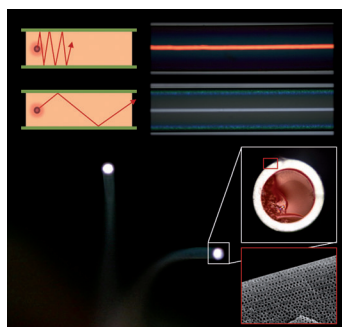


Squeezing out the energy: Macroscopically reversible deformation of polymers in contact with water produces H_2O_2 in quantities that are sufficient to drive small-scale chemical syntheses. The amount of mechanosynthesized H_2O_2 scales with the polymer-water interfacial area, and the efficiency of the mechanical-to-chemical energy transduction can be as high as 30% for soft, porous polymer “sponges”.

Mechanochemistry

H. T. Baytekin, B. Baytekin, B. A. Grzybowski* ————— 3596 – 3600

Mechanoradicals Created in “Polymeric Sponges” Drive Reactions in Aqueous Media



Photonic crystal fibers have been created using the spontaneous crystallization of colloidal particles in a photocurable resin coated on the inner wall of microcapillaries. The controlled deposition of films on the microcapillaries allows the thickness and number of layers in the photonic crystal fibers to be controlled. A stop band in a colloidal photonic crystal fiber can enhance the efficiency of light guidance (see picture).

Photonic Crystals

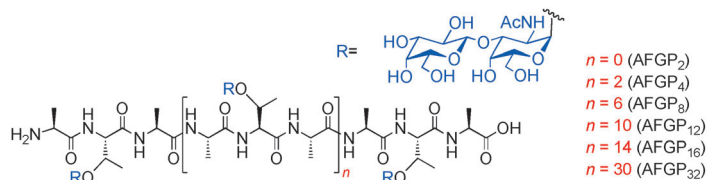
S.-H. Kim,* H. Hwang, S.-M. Yang* ————— 3601 – 3605

Fabrication of Robust Optical Fibers by Controlling Film Drainage of Colloids in Capillaries



Peptide Ligations

B. L. Wilkinson, R. S. Stone,
C. J. Capicciotti, M. Thaysen-Andersen,
J. M. Matthews, N. H. Packer, R. N. Ben,
R. J. Payne* ————— 3606–3610



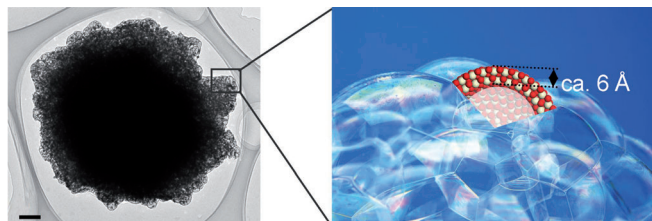
Total Synthesis of Homogeneous
Antifreeze Glycopeptides and
Glycoproteins

Don't freeze! A native chemical ligation–
desulfurization strategy has been
employed for the convergent synthesis of
a library of defined antifreeze glycopep-
tides and glycoproteins (AFGPs) ranging

in size from 1.2 to 19.5 kDa (see picture).
These AFGPs possessed the secondary
structure of a polyproline type II helix and
exhibited significant ice recrystallization
inhibition and thermal hysteresis activity.

Ceria Foams

J. Xing, H. F. Wang, C. Yang, D. Wang,
H. J. Zhao, G. Z. Lu, P. Hu,
H. G. Yang* ————— 3611–3615



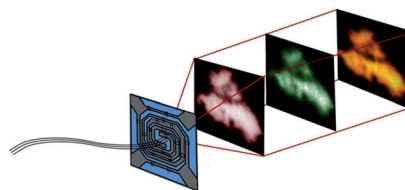
Ceria Foam with Atomically Thin Single-
Crystal Walls

All in a lather: A three-dimensional CeO₂
foam with long-range ultrathin (4–8 Å)
single-crystalline walls was synthesized
successfully by thermal decomposing
CeGeO₄ crystals under an NH₃ atmos-

phere. First-principles calculations were
also performed to understand the feasi-
bility and reaction pathways of thermal
decomposition of CeGeO₄. Scale bar:
200 nm.

Zeolite Catalysis

L. R. Aramburo, E. de Smit, B. Arstad,
M. M. van Schooneveld, L. Sommer,
A. Juhin, T. Yokosawa, H. W. Zandbergen,
U. Olsbye, F. M. F. de Groot,
B. M. Weckhuysen* ————— 3616–3619

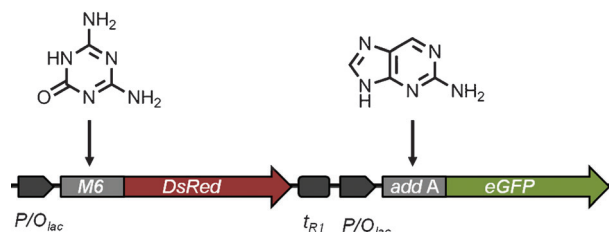


X-ray Imaging of Zeolite Particles at the
Nanoscale: Influence of Steaming on the
State of Aluminum and the Methanol-To-
Olefin Reaction

Zeolites in the spotlight: A combination of
scanning transmission X-ray microscopy
(see picture) and bulk methods give
nanoscale chemical insight in the distri-
bution of Al and C within ZSM-5 zeolites
during methanol-to-olefin reactions. The
distinct catalyst performances could be
related to differences in the spatial dis-
tribution of the hydrocarbons.

Riboswitches

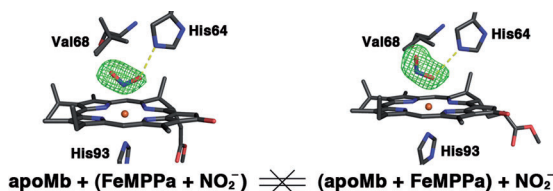
N. Dixon, C. J. Robinson, T. Geerlings,
J. N. Duncan, S. P. Drummond,
J. Micklefield* ————— 3620–3624



Orthogonal Riboswitches for Tuneable
Coexpression in Bacteria

Orthogonal gene control: Orthogonal ri-
boswitches can be deployed in the same
bacterial cell to independently control the
coexpression of multiple genes in a dose-
dependent response to distinct synthetic

small molecules. This technique allows
convenient access to highly dynamic
expression landscapes and desirable pro-
tein stoichiometries.



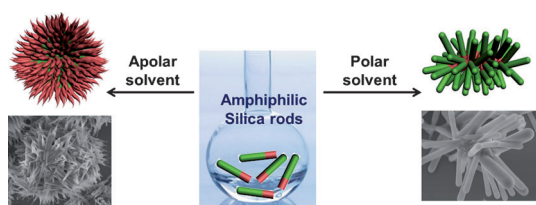
Who is in charge? Nitrite linkage isomerism in the same heme protein occurs as a function of the compound preparation method. An N-bound nitrite conformation is achieved when a pre-formed iron chlorin–nitrite model compound is

inserted into apoMb. In contrast, an O-bound nitrite conformation is evident when nitrite is added to the chlorin-substituted Mb. The results suggest that the Mb distal pocket is in charge of directing the ligand binding mode.

Linkage Isomerism

J. Yi,* L. M. Thomas,
G. B. Richter-Addo* 3625–3627

Distal Pocket Control of Nitrite Binding in Myoglobin



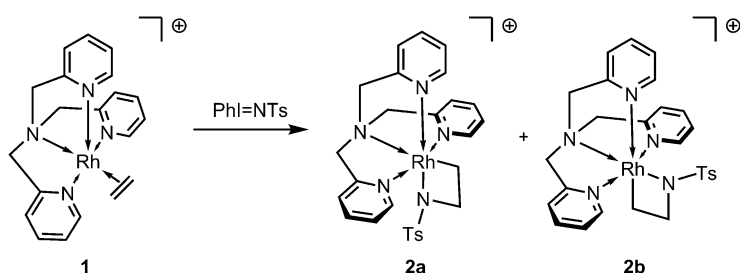
Flowers and stars: A wet-chemical method was developed to synthesize amphiphilic rodlike silica particles with hydrophilic (green in picture) and hydrophobic (red) blocks. The self-assembly of the amphiphilic rodlike particles leads to

various structures including planar monolayers, bundle micelles, flower micelles, star micelles (right in picture), and reverse micelles (left) depending on the properties of the rods and the nature of the solvent.

Colloidal Particles

J. He, B. Yu, M. J. Hourwitz, Y. Liu,
M. T. Perez, J. Yang, Z. Nie* 3628–3633

Wet-Chemical Synthesis of Amphiphilic Rodlike Silica Particles and their Molecular Mimetic Assembly in Selective Solvents



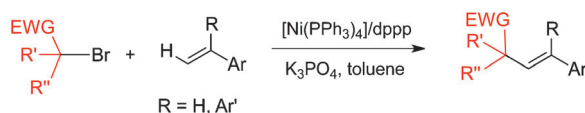
AmAZing metallacycles: Azarhodacyclobutane was prepared by oxidation of Rh^I–olefin complex **1** (see Scheme; Ts = *p*-toluenesulfonyl). Both isomers **2a** and **2b**

were isolated and characterized by NMR spectroscopy and mass spectrometry; their configurations were unambiguously established by NOE experiments.

Metallacyclobutanes

A. Dauth, J. A. Love 3634–3637

Preparation of 2-Azarhodacyclobutanes by Rhodium(I)–Olefin Oxidation



Ni made it! A novel Heck-type reaction of secondary and tertiary α -carbonyl alkyl bromides, most likely involving a radical process, was achieved through the use of a nickel catalyst. Various substituted styrenes and 1,1-diaryl alkenes were utilized

as substrates to easily construct α -alkenyl carbonyl compounds with tertiary or quaternary carbon centers. A catalytic cycle involving Ni^I/Ni^{II} is proposed based on our experimental results. EWG = electron-withdrawing group.

Cross-Coupling

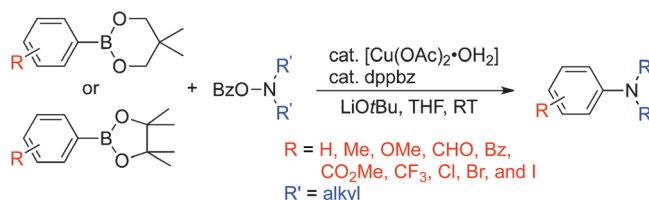
C. Liu, S. Tang, D. Liu, J. Yuan, L. Zheng,
L. Meng, A. Lei* 3638–3641

Nickel-Catalyzed Heck-Type Alkenylation of Secondary and Tertiary α -Carbonyl Alkyl Bromides



Synthetic Methods

N. Matsuda, K. Hirano,* T. Satoh,
M. Miura* 3642–3645



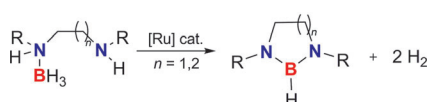
Copper-Catalyzed Amination of
Arylboronates with *N,N*-
Dialkylhydroxylamines

A tolerant coupling: The title reaction has been developed to deliver arylamines (see scheme; Bz = benzoyl, dppbz = 1,2-bis-(diphenylphosphino)benzene). The catalysis is based on electrophilic, umpolung

amination and enables the use of secondary acyclic amines. Various functional groups are tolerated, thus opening up a new substrate class for the Chan–Lam-type coupling.

Homogeneous Catalysis

C. J. Wallis, H. Dyer, L. Vendier,
G. Alcaraz,*
S. Sabo-Etienne* 3646–3648

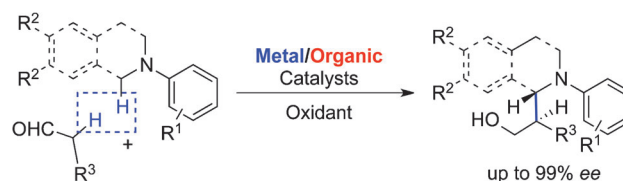


Dehydrogenation of Diamine–
Monoboranes to Cyclic Diaminoboranes:
Efficient Ruthenium-Catalyzed
Dehydrogenative Cyclization

Remote control: The title reaction is the first example of a catalyzed dehydrogenative cyclization (CDC) of diamine–monoboranes to give cyclic diaminoboranes. The cyclization reaction is strongly dependent on the nature of the substitution pattern at the remote amino group.

Synthetic Methods

J. Zhang, B. Tiwari, C. Xing, X. Chen,
Y. R. Chi* 3649–3652



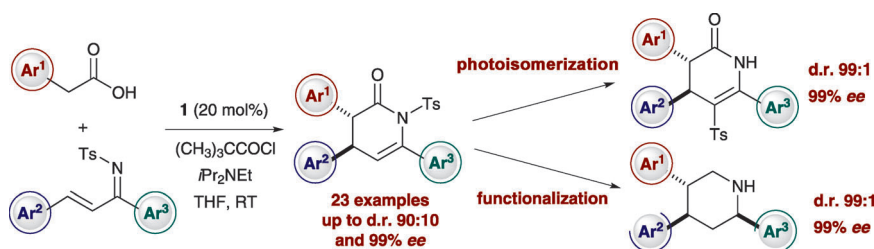
Enantioselective Oxidative Cross-
Dehydrogenative Coupling of Tertiary
Amines to Aldehydes

Cooperative catalysts: An enantioselective and direct oxidative coupling of aldehydes to tertiary amines to give β -amino alcohols is described. Catalyzed by copper(II), the reaction proceeds to give a racemic

mixture of products; however, by using a combination of copper(II) and a chiral amine catalyst, the reaction gives the desired products with high enantioselectivity (see scheme).

Asymmetric Catalysis

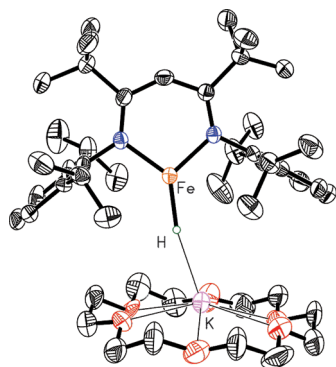
C. Simal, T. Lebl, A. M. Z. Slawin,
A. D. Smith* 3653–3657



Dihydropyridones: Catalytic Asymmetric
Synthesis, *N*- to *C*-Sulfonyl Transfer, and
Derivatizations

Benzotetramisole (1) promotes the reaction of ammonium enolates derived from arylacetic acids with *N*-tosyl- α,β -unsaturated ketimines, thus giving dihydropyridones with high diastereo- and enantio-

control (see scheme). These products readily undergo *N*- to *C*-sulfonyl photoisomerization and are derivatized to afford stereodefined piperidines and tetrahydropyrans.

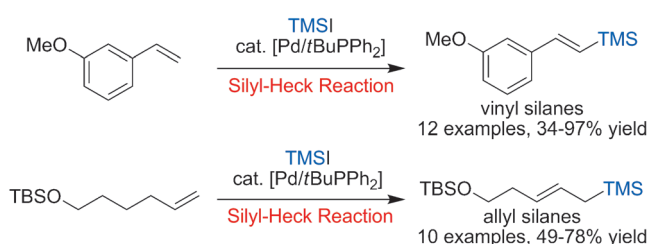


Three's company: Iron(II) hydride complexes are presented (see picture; N blue, O red) that are the first monomeric open-shell hydride complexes to be crystallographically verified as being three-coordinate at the metal. Backbonding into diketiminate π^* orbitals stabilizes the low oxidation state. The Fe–H bonding has been analyzed using electron-nuclear double resonance (ENDOR).

Hydrides in Biology

K. P. Chiang, C. C. Scarborough, M. Horitani, N. S. Lees, K. Ding, T. R. Dugan, W. W. Brennessel, E. Bill,* B. M. Hoffman,*
P. L. Holland* ————— 3658–3662

Characterization of the Fe–H Bond in a Three-Coordinate Terminal Hydride Complex of Iron(II)



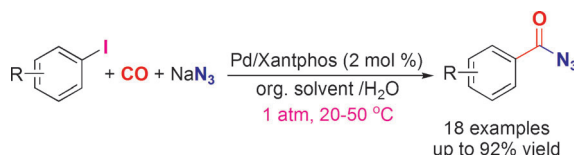
Installing silicon is easy! A high-yielding protocol for the palladium-catalyzed silylation of terminal alkenes is reported. This method allows facile conversion of styrenes to *E*- β -silyl styrenes by using iodo-

trimethylsilane (TMSI) or chlorotrimethylsilane/lithium iodide (see scheme). Terminal allyl silanes with good *E/Z* ratios are also readily accessed from α -olefins.

Synthetic Methods

J. R. McAtee, S. E. S. Martin, D. T. Ahneman, K. A. Johnson, D. A. Watson* ————— 3663–3667

Preparation of Allyl and Vinyl Silanes by the Palladium-Catalyzed Silylation of Terminal Olefins: A Silyl-Heck Reaction



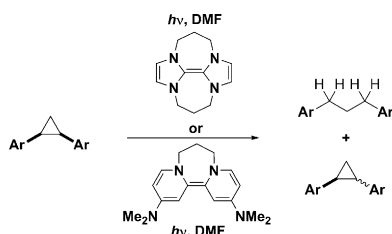
Aryl iodides smoothly react with NaN_3 and CO in the presence of a Pd/Xantphos catalyst to give aryl azides (ArCON_3) in 75–92% yield. The reaction occurs under

mild reaction conditions (1 atm, 20–50 °C) and exhibits high functional-group tolerance. (Xantphos = 9,9-dimethyl-4,5-bis(diphenylphosphino)xanthene)

Azidocarbonylation

F. M. Miloserdov, V. V. Grushin* ————— 3668–3672

Palladium-Catalyzed Aromatic Azidocarbonylation



Powerful reduction reactions: Simple organic electron donors, composed solely of the elements carbon, hydrogen, and nitrogen, reduce ground-state benzene rings to their radical anions by electron transfer upon photoactivation (DMF = dimethylformamide).

Reduction of Benzenes

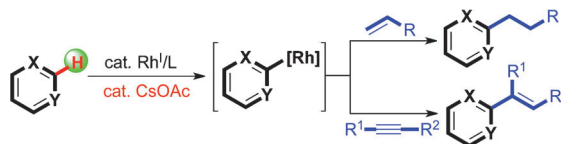
E. Cahard, F. Schoenebeck,* J. Garnier, S. P. Y. Cutulic, S. Zhou, J. A. Murphy* ————— 3673–3676

Electron Transfer to Benzenes by Photoactivated Neutral Organic Electron Donor Molecules



Hydroheteroarylation

J. Ryu, S. H. Cho,*
S. Chang* 3677–3681



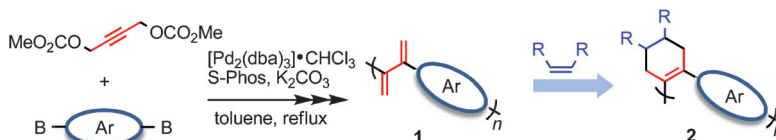
A Versatile Rhodium(I) Catalyst System for the Addition of Heteroarenes to both Alkenes and Alkynes by a C–H Bond Activation

Rhod to Addition: A highly efficient and convenient rhodium catalyst system was developed for the title transformation. A base co-catalyst was found to facilitate the key arene C–H bond-activation step and substrate scope was very broad, including

both electron-deficient pyridine *N*-oxides, and electron-rich azoles. The catalytic system was effective for the hydroheteroarylation of both alkenes and alkynes and gave excellent regio- and stereoselectivity.

Polymerization

N. Nishioka, S. Hayashi,
T. Koizumi* 3682–3685



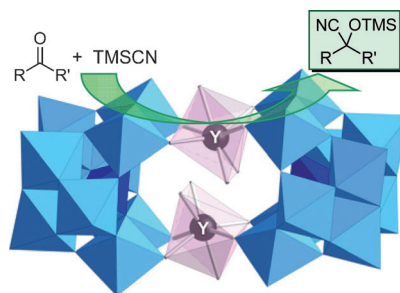
Palladium(0)-Catalyzed Synthesis of Cross-Conjugated Polymers: Transformation into Linear-Conjugated Polymers through the Diels–Alder Reaction

Making the shift: The title reaction of a propargylic bis(carbonate) with diboron compounds leads to new cross-conjugated polymers **1** having 2,3-butadienylene moieties. **1** is then converted into the linear-conjugated polymers **2** through

a Diels–Alder reaction. The fluorescent spectra of the *cis*-linked polymers **2** show large Stokes shifts compared to those of the cross-conjugated polymer precursors **1**.

Polyoxometalates

Y. Kikukawa, K. Suzuki, M. Sugawa,
T. Hirano, K. Kamata, K. Yamaguchi,
N. Mizuno* 3686–3690

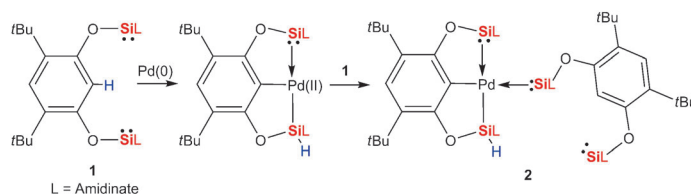


Cyanosilylation of Carbonyl Compounds with Trimethylsilyl Cyanide Catalyzed by an Yttrium-Pillared Silicotungstate Dimer

An yttrium-pillared silicotungstate dimer (see picture) catalyzes the cyanosilylation of structurally diverse ketones and aldehydes with trimethylsilyl cyanide (TMSCN). The reactions proceed selectively and afford the corresponding cyanohydrin trimethylsilyl ethers. The catalytic performance is significant, in particular for aldehydes, with a turnover number of 18 000 and a turnover frequency of 540 000 h^{−1} for *n*-hexanal.

Coordination Chemistry

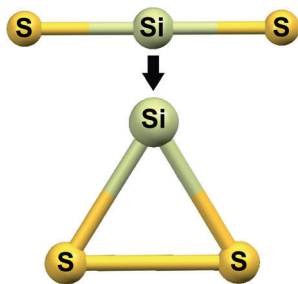
W. Wang, S. Inoue,* E. Irran,
M. Driess* 3691–3694



Synthesis and Unexpected Coordination of a Silicon(II)-Based SiCSi Pincerlike Arene to Palladium

SiCSi to pick up a metal: A bis(silylene) SiCSi pincerlike arene **1** (see scheme) has been synthesized through salt metathesis reaction of the dilithium salt of 2,4-di-*tert*-butyl-resorcinolate with the respective

chloro silylene precursor [LSiCl]. Remarkably, **1** reacts with Pd(PPh₃)₄ in a molar ratio of 2:1 under loss of all phosphine ligands to give the pincer complex **2**.



A joint effort: By means of high-resolution rotational spectroscopy and highly accurate quantum-chemical calculations, the first observation and characterization of cyclic SiS_2 was achieved. This provides a new perspective on the Walsh rules: Although the cyclic form of SiS_2 is a local and not the global minimum, cyclic isomers of sixteen-electron triatomics containing second or even higher row elements are experimentally accessible.

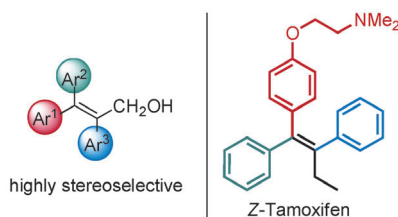
Small-Ring Systems

L. A. Mück,* V. Lattanzi, S. Thorwirth, M. C. McCarthy, J. Gauss — **3695–3698**

Cyclic SiS_2 : A New Perspective on the Walsh Rules



One, two, and three! Nitroxides and dioxygen serve as oxidants in highly stereoselective oxidative Pd-catalyzed Heck arylations in which aryl boronic acids are used to synthesize triarylalkyl-substituted olefins. The reactions occur



under very mild conditions at room temperature. As an example, the threefold sequential arylation of methyl acrylate is the crucial step in the stereoselective synthesis of Z-Tamoxifen.

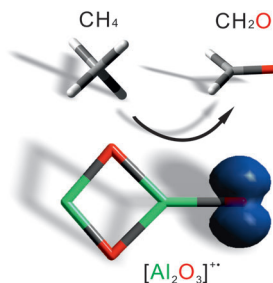
Oxidative Olefin Arylation

Z. He, S. Kirchberg, R. Fröhlich, A. Studer* — **3699–3702**

Oxidative Heck Arylation for the Stereoselective Synthesis of Tetrasubstituted Olefins Using Nitroxides as Oxidants



Just one step: Reactivity studies demonstrate that in the gas phase $[\text{Al}_2\text{O}_3]^+$ clusters can efficiently conduct the direct conversion of CH_4 into CH_2O at room temperature (see scheme). The reaction mechanism is highly complex involving oxygen-atom transfer and a double hydrogen-atom transfer.

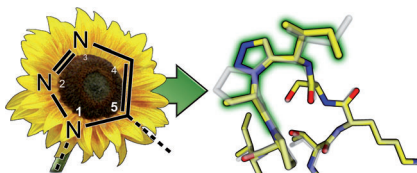


Methane Activation

Z.-C. Wang, N. Dietl, R. Kretschmer, J.-B. Ma, T. Weiske, M. Schlangen,* H. Schwarz* — **3703–3707**

Direct Conversion of Methane into Formaldehyde Mediated by $[\text{Al}_2\text{O}_3]^+$ at Room Temperature

Flower power: Potent protease inhibitors containing triazolyl mimics of *cis* and *trans* backbone amides were engineered based on the structure of the sunflower trypsin inhibitor 1. The biologically relevant *cis*-Pro motif was successfully replaced with a non-prolyl unit. High-resolution crystal structures of 1,4- and 1,5-disubstituted 1,2,3-triazolyl peptidomimetics can serve in the design of tailor-made Bowman–Birk inhibitors.



Amide Mimics

M. Tischler, D. Nasu, M. Empting, S. Schmelz, D. W. Heinz, P. Rottmann, H. Kolmar, G. Buntkowsky,* D. Tietze,* O. Avrutina* — **3708–3712**

Braces for the Peptide Backbone: Insights into Structure–Activity Relationships of Protease Inhibitor Mimics with Locked Amide Conformations

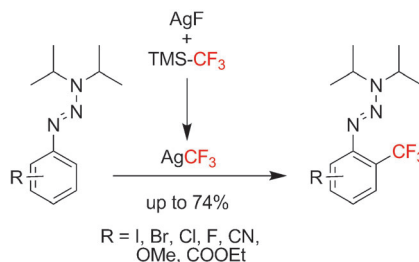


Trifluoromethylation

A. Hafner, S. Bräse* — 3713–3715



Ortho-Trifluoromethylation of
Functionalized Aromatic Triazenes



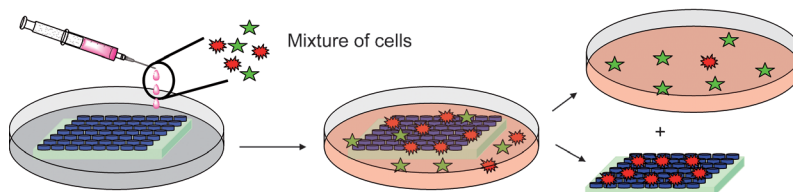
A silver key to add CF₃: In presence of in situ generated AgCF₃, it is possible to trifluoromethylate aromatic triazenes in high *ortho* selectivity and good yields by means of a C–H substitution (see scheme). Owing to the further transformation possibilities offered by triazenes, a variety of CF₃-substituted building blocks are then accessible.

Selective Cell Adhesion

J. El-Gindi, K. Benson, L. De Cola,
H.-J. Galla, N. Seda Kehr* — 3716–3720



Cell Adhesion Behavior on
Enantiomerically Functionalized Zeolite L
Monolayers



Zeolite L nanocrystals can be enantioselectively functionalized and their enantiomorphous SAMs prepared. The adhesion behavior of different cells with these new biomaterials was studied according

to the respective surface chirality. This concept was demonstrated for cell separation of primary cells and cell lines (see picture).



Supporting information is available
on www.angewandte.org
(see article for access details).



A video clip is available as Supporting
Information on www.angewandte.org
(see article for access details).



This article is available
online free of charge
(Open Access).



This article is accompanied by a cover picture (front or back cover, and inside or outside).

Sources

Product and Company Directory

You can start the entry for your company in “Sources” in any issue of *Angewandte Chemie*.

If you would like more information, please do not hesitate to contact us.

Wiley-VCH Verlag – Advertising Department

Tel.: 0 62 01 - 60 65 65

Fax: 0 62 01 - 60 65 50

E-Mail: MSchulz@wiley-vch.de

Service

Spotlight on Angewandte's

Sister Journals — 3510–3512

Preview — 3722